Journal of Cellular Physiology

DEFICIENT MUSCLE REGENERATION POTENTIAL IN SARCOPENIC COPD PATIENTS: ROLE OF SATELLITE CELLS

Journal:	*Journal of Cellular Physiology*
Manuscript ID	Draft
Wiley - Manuscript type:	Original Research Article
Date Submitted by the Author:	n/a
Complete List of Authors:	Sancho-Munoz, Antonio; IMIM-Hospital del Mar, Parc de Salut Mar, UPF Guitart, Maria; IMIM-Hospital del Mar, Parc de Salut Mar, UPF, CIBERES Rodriguez, Diego; IMIM-Hospital del Mar, Parc de Salut Mar, UPF, CIBERES Gea, Joaquim; IMIM-Hospital del Mar, Universitat Pompeu Fabra, Barcelona Biomedical Research Park (PRBB), Respiratory Medicine Martinez-Llorens, Juana; IMIM-Hospital del Mar, Parc de Salut Mar, UPF, CIBERES Barreiro, Esther; IMIM-Hospital del Mar, UPF, PRBB, CIBERES, Pulmonology-URMAR
Key Words:	COPD, lower limb muscles, muscle regeneration markers, myostatin, satellite cells

DEFICIENT MUSCLE REGENERATION POTENTIAL IN SARCOPENIC COPD PATIENTS: ROLE OF SATELLITE CELLS

Antonio Sancho-Muñoz[1], Maria Guitart[1,2], Diego A Rodríguez[1,2], Joaquim Gea[1,2], Juana Martínez-Llorens[1,2], Esther Barreiro[1,2]

[1]Pulmonology Department-Muscle Wasting and Cachexia in Chronic Respiratory Diseases and Lung Cancer Research Group, IMIM-*Hospital del Mar, Parc de Salut Mar*, Health and Experimental Sciences Department (CEXS), *Universitat Pompeu Fabra* (UPF), Barcelona Biomedical Research Park (PRBB), Dr. Aiguader, 88, E-08003 Barcelona.

[2]*Centro de Investigación en Red de Enfermedades Respiratorias* (CIBERES), *Instituto de Salud Carlos III* (ISCIII), Monforte de Lemos, 5, E-28029 Madrid.

Corresponding author: Dr. Esther Barreiro, Pulmonology Department-Pulmonology Department, Muscle Wasting & Cachexia in Chronic Respiratory Diseases & Lung Cancer Research Group, IMIM-Hospital del Mar, PRBB, Dr. Aiguader, 88, E-08003 Barcelona, Spain, Telephone: +34 93 316 0385, Fax: +34 93 316 0410, e-mail: ebarreiro@imim.es

Short title: Muscle regeneration in COPD sarcopenia

Word count: 6,508

Data availability statement: The data sets used and/or analyzed during the current study are available from the corresponding author on reasonable request.

ACKNOWLEDGEMENTS

The authors gratefully acknowledge the help provided by MSc Kseniya Ihnatsiuk with part of the molecular experiments, MSc Mireia Admetlló, Ana Balañá, and Anna Rodó for their help with patient recruitment and evaluation. The current research has been supported by FIS 18/00075 & CIBERES (FEDER, ISC-III), SEPAR 2018, and VIFOR Pharma 2018.

ABSTRACT

Sarcopenia is a major comorbidity in COPD. Whether deficient muscle repair mechanisms and regeneration exists in vastus lateralis (VL) of sarcopenic COPD remains debatable. In vastus lateralis (VL) of control subjects and severe COPD patients with/without sarcopenia, satellite cells (SCs) were identified (immunofluorescence, specific antibodies, anti-Pax-7 and anti-Myf-5): activated (Pax-7+/Myf-5+), quiescent/regenerative potential (Pax-7+/Myf-5-), and total SCs, nuclear activation (TUNEL), and muscle fiber type (morphometry and slow- and fast-twitch, and hybrid fibers), muscle damage (hematoxylin-eosin staining), muscle regeneration markers (Pax-7, Myf-5, myogenin, and MyoD), and myostatin levels were identified. Compared to controls, in VL of sarcopenic COPD patients, myostatin content, activated SCs, hybrid fiber proportions, TUNEL-positive cells, internal nuclei, and muscle damage significantly increased, while quadriceps muscle strength, numbers of Pax-7+ /Myf-5- and slow- and fast-twitch, and hybrid myofiber areas decreased. In VL of sarcopenic and non-sarcopenic patients, TUNEL-positive cells were greater, whereas muscle regeneration marker expression was lower than in controls. In VL of severe COPD patients regardless of the sarcopenia level, muscle regeneration process is triggered as identified by satellite cell activation and increased internal nuclei. Nonetheless, a lower regenerative potential along with significant alterations in muscle phenotype and damage, and increased myostatin were prominently seen in sarcopenic COPD.

Word count: 200

KEY WORDS: COPD; lower limb muscles; muscle regeneration markers; myostatin; satellite cells

INTRODUCTION

Sarcopenia is a major comorbidity commonly associated with chronic respiratory diseases including COPD. The reduction of muscle mass and strength of the lower limbs differs vastly from that taking place in the respiratory muscles (Esther Barreiro, 2019; Gea & Martínez-Llorens, 2019; Gea et al., 2019; Jaitovich & Barreiro, 2018). Sarcopenia limits the exercise capacity of the patients, thus having a negative impact on their daily-life activities and quality of life (Kwan et al., 2019; Shrikrishna et al., 2012). Furthermore, sarcopenia predicts death for the same degree of disease severity as measured by the level of the airway obstruction (Marquis et al., 2002; Swallow et al., 2007).

In the multifactorial etiology of sarcopenia associated with COPD, several clinical factors and conditions inherent to the respiratory disease, namely deconditioning, exert deleterious effects on the limb muscles through biological events and mechanisms as previously reported in relevant investigations. Most of the investigations have focused on the elucidation of factors and mechanisms primarily involved in the process of muscle mass loss in the limb muscles of the patients (E. Barreiro, Sznajder, Nader, & Budinger, 2015; Esther Barreiro, 2019; Gea & Martínez-Llorens, 2019; Gea et al., 2019; Jaitovich & Barreiro, 2018) and animal models (Chacon-Cabrera et al., 2014; Chacon-Cabrera, Lund-Palau, Gea, & Barreiro, 2016). Nonetheless, few studies have addressed the issue of the ability of the skeletal muscles to regenerate, let alone in muscles of COPD patients. The regenerative potential of a muscle will determine its capacity to regenerate following injury.

The progenitor myoblasts fuse during development to form skeletal muscles. Under normal conditions, in adult muscles, sporadic fusion of satellite cells, defined as postnatal muscle stem cells, takes place to replace the muscle turnover related to daily life activity. As skeletal muscle has the ability to regenerate following injury, regeneration of muscle tissue is a very fine regulated process in adults. The interaction between satellite cells and the

microenvironment are the basis of muscle regeneration. As such, satellite cell numbers have been shown to be modified under specific conditions such as in aging (Suetta et al., 2013), disuse muscle atrophy (Snijders et al., 2014), prolonged bed rest (Arentson-Lantz, English, Paddon-Jones, & Fry, 2016), and exposure to cigarette smoking (Chan et al., 2020). These modifications may alter the process of muscle regeneration in those conditions, which in turn, may coincide in patients with respiratory diseases such as in COPD.

The population of satellite cells is not homogeneous. Indeed, it has been proposed that satellite cells are heterogeneous populations of stem cells and committed progenitor cells that play different roles in the process of muscle regeneration. The activity of the skeletal muscle influenced the numbers of satellite cells in different models. For instance, aging hampered muscle regrowth following a period of disuse muscle atrophy in healthy humans (Suetta et al., 2013). In middle-aged adults, a decline in satellite cell counts was observed in the atrophic muscles following a 14-day period of bed rest (Arentson-Lantz et al., 2016). Nonetheless, changes in satellite cell counts were not detected in the quadriceps muscle of healthy young subjects following a two-week period of one-legged knee immobilization (Snijders et al., 2014).

Importantly, in the intercostal muscles of severe COPD patients, activation of satellite cells along with microstructural changes were detected (Martínez-Llorens et al., 2008). However, muscle regeneration and satellite cell counts were reduced in the vastus lateralis (VL) of patients with COPD with preserved body composition (Menon et al., 2012; M.-E. Thériault, Paré, Lemire, Maltais, & Debigaré, 2014; M. E. Thériault, Paré, Maltais, & Debigaré, 2012). Whether muscle regeneration events and satellite cell counts and types may differ in the lower limb muscles of patients with a different degree of disease severity and/or body composition remains to be fully elucidated.

Myostatin is a potent negative regulator of muscle mass in mammals. Myostatin keeps

the quiescence of satellite cells, whereas its absence triggers activation of satellite cells. Deletion of myostatin gene favors muscle mass and may lead to muscle hypertrophy (Ohno et al., 2016). Moreover, myostatin blockade elicited an improvement in the regenerative potential of limb muscles of mice following cardiotoxin-induced injury (Ohno et al., 2016). Recently, it has also been demonstrated that myostatin plays a key role in sarcopenia and it was suggested that its blockade improved muscle regeneration following injury (Scimeca et al., 2017). Moreover, myostatin inhibition reduced muscle atrophy through upregulation of markers involved in muscle regeneration in limb muscles of rats (Wurtzel et al., 2017).

On this basis, we hypothesized that the muscle regenerative potential as measured by the number of stem cells and other markers of muscle regeneration may be altered in the quadriceps of patients with COPD, especially in those with sarcopenia. Furthermore, protein levels of the potent negative regulator of muscle regeneration myostatin were also assessed in the VL of sarcopenic COPD patients. Accordingly, the study objectives were that in the vastus lateralis of severe COPD patients with a wide range of body composition, including those with sarcopenia, the following events were analyzed: 1) identification and counts of stem cells (regenerative potential) and committed progenitors, 2) markers of muscle regeneration and myostatin, and 3) muscle structural abnormalities and phenotype. A group of control subjects was also recruited for the purpose of the investigation, in whom muscle biopsies were also obtained and analyzed accordingly.

METHODS

Study design and population

This was a prospective, controlled, cross-sectional study, in which 45 patients (25 males) with stable COPD (Miravitlles et al., 2017; Vogelmeier et al., 2017) were recruited consecutively from the COPD clinics of the Respiratory Department at Hospital del Mar (Barcelona) over

the years 2018-2019. Additionally, 13 age-matched control subjects (6 males) were recruited from the general population (patients' relatives or friends) at Hospital del Mar. COPD patients were further subdivided into those with and without loss of muscle mass and strength (sarcopenic COPD, n=26, 11 males and non-sarcopenic COPD, n=19, 14 males) following the international consensus criteria on muscle wasting and sarcopenia (Cao & Morley, 2016; Muscaritoli et al., 2010) and previously published criteria (Esther Barreiro, Salazar-Degracia, Sancho-Muñoz, & Gea, 2019; Puig-Vilanova, Martínez-Llorens, et al., 2015).

In all patients, reduced muscle mass was defined as a fat-free mass index (FFMI) ≤ 18 kg/m^2, cut-off value established for a Mediterranean population in accordance with both previously published criteria (Esther Barreiro et al., 2019; Puig-Vilanova, Martínez-Llorens, et al., 2015) and the international consensus on the definition of sarcopenia (Cao & Morley, 2016; Muscaritoli et al., 2010). Moreover, muscle weakness was defined on the basis of previous investigations (approximately 25% reduction in quadriceps force compared to that observed in control subjects) (Puig-Vilanova, Martínez-Llorens, et al., 2015; Seymour et al., 2010). Control subjects were never-smoker male and female sedentary control individuals recruited from the general population (patients' relatives or friends), while patients in both groups were active smokers or ex-smokers. All patients were on inhaled bronchodilators. They were clinically stable at the time of the study, without episodes of exacerbation or oral steroid treatment in the previous three months. None of them presented significant comorbidities. All groups of individuals were Caucasian.

Exclusion criteria. Exclusion criteria for COPD patients and control subjects included other chronic respiratory or cardiovascular disorders, acute exacerbations in the last three months, limiting osteoarticular condition, chronic metabolic diseases, suspected para-neoplastic or myopathic syndromes, and/or treatment with drugs known to alter muscle structure and/or function including oral corticosteroids. COPD patients and control subjects were qualified as

sedentary after being specifically inquired about whether they were conducting any regular outdoor physical activity, going regularly to the gymnasium, or participating in any specific training program. Specifically, sedentarism was defined on the basis of the following criteria: 1) if subjects were not engaged in one or more of these activities: walking, running, bike riding, swimming, dancing, gardening, or weight lifting more than five times per week, 2) not performing at least three hours/week of endurance-type physical activity, and/or 3) inactive general state in which leisure time physical activity was minimal (Ricciardi, 2006). Moreover, the time spent in sedentary postures (lying and sitting) was also considered in the assessment of sedentarism in the study groups (Ricciardi, 2006).

Ethics

The current investigation was designed in accordance with both the ethical standards on human experimentation in our institution and the World Medical Association guidelines (Seventh revision of the Declaration of Helsinki, Fortaleza, Brazil, 2013) (Shrestha & Dunn, 2020) for research on human beings. Approval was obtained from the institutional Ethics Committee on Human Investigation (*Hospital del Mar-IMIM,* Barcelona, project number 2018/7937/I). Informed written consent was obtained from both patients and control subjects.

Anthropometric and functional assessment

Anthropometric evaluation included body mass index (BMI) and determination of FFMI using bioelectrical impedance (Esther Barreiro et al., 2019; Puig-Vilanova, Martínez-Llorens, et al., 2015). Nutritional parameters were also evaluated through conventional blood tests. Diagnostic criteria for sarcopenia were BMI < 21 kg/m^2 and FFMI < 18 kg/m^2 in all patients (Esther Barreiro et al., 2019; Coin et al., 2008; Puig-Vilanova, Martínez-Llorens, et al., 2015). Lung function was evaluated through determination of spirometry, static lung volumes, diffusion capacity, and blood gases using standard procedures and well-established reference

values (Roca, Burgos, Barberà, et al., 1998; Roca, Burgos, Sunyer, et al., 1998; Roca et al., 2014).

Quadriceps muscle strength was evaluated in both patients and controls through the determination of the isometric maximum voluntary contraction (QMVC) of the dominant lower limb as formerly described (Esther Barreiro et al., 2019; Puig-Vilanova, Martínez-Llorens, et al., 2015). Briefly, patients were seated with both trunk and thigh fixed on a rigid support of an exercise platform (Domyos HGH 050, Decathlon, Lille, France). The highest value from three brief reproducible maneuvers (<5% variability among them) was accepted as the QMVC.

Exercise capacity. Exercise capacity was assessed through the six-minute walking distance following previous methodologies (Rodriguez et al., 2012). The test consisted of two attempts (with at least a 30-minute rest between them) in a 30-meter corridor. Encouragement was given every minute and the test was interrupted if symptoms of exhaustion appeared. A modified Borg scale was used to quantify the levels of dyspnea and legs discomfort.

Maximum exercise capacity was also measured using standardized incremental on a cycloergometer (Jones, Makrides, Hitchcock, Chypchar, & McCartney, 1985; Rodriguez et al., 2012). Pulmonary gas exchange and ventilatory measurements were obtained from calibrated signals derived from rapid response gas analyzer and a mass flow sensor. Oxygen uptake (VO_2), pulmonary carbon dioxide output (VCO_2), minute ventilation (VE), respiratory exchange ratio (RER) were also registered during each respiration. Heart rate (HR) was determined using a ten-lead online electrocardiogram and oxygen saturation by pulse oximetry (SpO_2). After one minute of breathing at rest, subjects pedaled on an electrically braked cycloergometer (Ergoline Ergometrix 900, Uberprüfung, Germany) (Jones et al., 1985; Rodriguez et al., 2012). An integrated computer recorded cardiorespiratory variables during

the test (Ultima, MedGraphics Corporation, St. Paul, MN, USA). Patients were encouraged to continue until they could no longer sustain the target pedaling load.

Blood samples and muscle biopsy

Patients and control subjects rested for one hour on a chair with legs half-flexed, time at which blood samples were obtained, after an overnight fasting period, right before initiation of the surgical procedures (Esther Barreiro et al., 2019; Puig-Vilanova, Martínez-Llorens, et al., 2015). Specimens from the VL portion of the quadriceps muscle (50-100 mg average weight) were obtained from all subjects using the open biopsy technique as previously described (Esther Barreiro et al., 2019; Puig-Vilanova, Martínez-Llorens, et al., 2015). Muscle specimens were always cleaned out of any blood contamination with saline. They were immediately frozen in liquid nitrogen and stored in the –80ºC freezer (under permanent alarm control) for further analyses or immersed in an alcohol-formol bath for two hours to be thereafter embedded in paraffin. Frozen tissues were used for mRNA expression and immunoblotting techniques, while paraffin-embedded tissues were used for the assessment of structural modifications (immunohistochemical analysis).

Biological analyses

Muscle fiber counts and morphometry. Myosin heavy chain (MyHC) -I and -II isoforms were identified in paraffin sections (three-micrometer thick) from VL muscles corresponding to the three study groups. The following antibodies were used: anti-MyHC-I (ab11083, Abcam, Cambridge, UK) and anti-MyHC-II (ab51263, Abcam) antibodies. Myofibers positively stained appeared in brown color. The fibers positively stained with the two antibodies simultaneously were identified as the hybrid fibers. The cross-sectional area, calculated using the mean least diameter, and the proportions of type I, type II and of the hybrid fibers were estimated with the aid of a light microscope (Olympus BX 61, Olympus Corporation, Hamburg, Germany) coupled with an image-digitizing camera (Pixera Studio, version 1.0.4,

Pixera Corporation, Los Gatos, CA, USA) and a digital image processing software (ImageJ, version 2006.02.01, National Institutes of Health, Bethesda, MD, USA). In all study groups, the amount of fibers measured and counted in each muscle preparation ranged between 100 and 300 (Esther Barreiro et al., 2019; Puig-Vilanova, Martínez-Llorens, et al., 2015).

Muscle structure abnormalities. Three-micrometer paraffin-embedded sections from the muscle specimens of the three study groups were used to assess the proportions of muscle abnormalities (Esther Barreiro et al., 2019; Puig-Vilanova, Martínez-Llorens, et al., 2015). A grid of 63 point-intercepts (7 x 9 rectangular pattern was superimposed onto the image of the muscle cross section at a magnification of x400 under the light microscope (Olympus BX 61, Olympus Corporation) using an image digitizing camera (Olympus DP 71, Olympus Corporation). Each point-intercept was assigned to a specific category and entered into the software. Categories for point counting were defined as follows: 1) normal muscle, 2) internal nucleus, 3) inflammatory cell, 4) lipofuscin, 5) abnormal viable, 6) inflamed/necrotic, 7) vessel, and 0) no count. The area fraction for each category was defined as the percentage of points that fell on each of these traits relative to the total number of points superimposed on all viable fields (all features except for categories 0 and 7) of each cross section. The area fraction of normal muscle was equivalent to the proportions of points falling in category 1, while the area fraction of abnormal muscle was determined by calculation of the proportion of points included in the other categories (categories 2 to 6).

Terminal deoxynucleotidyl transferase-mediated dUTP nick-end labeling (TUNEL) assay. In three-micrometer paraffin-embedded sections of muscle specimens, activation of the myonuclei was determined using the TUNEL assay (ApopTag Peroxidase In Situ Apoptosis Detection Kit, Merck Millipore, Burlington, United States). The manufacturer's instructions and previously published studies were followed (E. Barreiro et al., 2011; Salazar-Degracia et al., 2016). In brief, during nuclear activation, fragments of genomic DNA can be generated.

These strand breaks in the DNA sequence can be identified by labeling 3'-OH terminal groups with modified nucleotides in an enzymatic reaction catalyzed by the terminal deoxynucleotidyl transferase (TdT) enzyme. Muscle sections were fixed, permeabilized and immediately incubated with the TUNEL Working Strength TdT Enzyme and the anti-Digoxigenin Conjugate. TdT catalyzed the adding of digoxigenin-dNTP at 3'-OH terminal groups in single- and double-stranded DNA. After washing, the sections were incubated with an anti-digoxigenin antibody conjugated with peroxidase, which resulted in brown color upon reaction. Negative control experiments, in which TdT enzyme was not added, were also performed. Apoptotic nuclei appeared in brown color, while negative nuclei were green (methyl green counterstaining). Only nuclei located within the muscle fiber boundary were counted in the study. Positive nuclei and the total number of nuclei were counted by two trained observers (correlation coefficient 95%). Apoptotic nuclei were expressed as the percentage of the TUNEL-positive nuclei to the total number of counted nuclei (E. Barreiro et al., 2011; Salazar-Degracia et al., 2016). A minimum of 300 nuclei were counted in each muscle specimen for all the study groups.

Satellite cell identification using immunofluorescence microscopy. Specific antibodies were used to detect quiescent, activated and total satellite cells using immunofluorescence as previously described (M. Guitart, Lloreta, Mañas-Garcia, & Barreiro, 2018). Briefly, three-micrometer paraffin sections of the muscle specimens of all study groups were deparaffinized and rehydrated by successive immersions in xylene, ethanol 100%, ethanol 90%, ethanol 70% and phosphate-buffered saline (PBS). A pressure cooker containing 10 mM citrate buffer (pH 6.0) was used to boil the sections for 20 minutes. Following a two-hour cooling period, sections were blocked with blocking solution (3% BSA, 10% goat serum, and 0.5% triton in PBS) for one hour. The sections were then incubated overnight at 4ºC with a mixture of two different primary antibodies: mouse monoclonal anti-Pax-7 IgG1k supernatant (1:20;

Developmental Studies Hybridoma Bank, Iowa, USA) and rabbit polyclonal anti-Myf-5 IgG (1:100, AVIVA systems, San Diego, USA), prepared in blocking solution. After incubation with the primary antibodies, the sections were incubated with the corresponding secondary antibodies at room temperature for one hour: Alexa Fluor® 488 AffiniPure goat anti-mouse IgG, Fcγ Subclass 1 Specific (1:800, Jackson Immunoresearch, West Grove, USA) and Alexa Fluor® plus 555 goat anti-rabbit IgG (H+L) (1:1000, Thermo Fisher Scientific, Waltham, USA) respectively, which were also prepared in blocking solution along with 4',6'-diamidino-2-phenylindole (DAPI) (1:1000). Finally, the sections were mounted using 70% glycerol in 30% PBS. A fluorescence microscope (Nikon Eclipse Ni, Nikon, Tokyo, Japan) at a magnification of x400 coupled with a digitizing camera was used to count the number of satellite cells. Anti-Pax-7 antibody alone was used to detect quiescent satellite cells, while the combination of anti-Pax-7 and anti-Myf-5 antibodies detected committed satellite cells (M. Guitart et al., 2018). The addition of quiescent and committed satellite cells corresponded to the total number of satellite cells. Results are expressed as follows: 1) Pax-7+/Myf-5- quiescent satellite cells, 2) Pax-7+/Myf-5+ activated satellite cells and 3) the addition of both types of cells identified as total satellite cells. All types of fibers were normalized by the number of myofibers counted within the ten fields analyzed in each muscle preparation. The number of counted satellite cells ranged from 25 to 144 (quiescent), from 0 to 38 (activated), and from 31 to 165 (total satellite cells) for the ten fields counted in each muscle preparation in a similar fashion in the three study groups.

RNA isolation. Snap-frozen muscle specimens were used to isolate total RNA using Trizol reagent (Life technologies, Carlsbad, California, USA). Fifty mg of muscle samples diluted in 1 mL of Trizol reagent were homogenized using a T10 basic Ultra-Turrax Polytron (IKA®-Werke GmbH & Co. KG, Staufen, Germany) at maximum speed for 20 seconds. The homogenized samples were incubated for a short period (10 minutes) at room temperature to

allow the nuclear proteins to dissociate. Subsequently, 0.2 mL chloroform were added to the samples, which were vigorously shaken manually for 15 seconds to be incubated at room temperature for three minutes. The samples were centrifuged at 12,000 g at 4 °C for 15 minutes. The centrifugation process separated the homogenates into a lower red organic phase and a white interphase, and a color-less upper aqueous phase. RNA content remained in the aqueous phase. The RNA-containing aqueous phase was transferred to a fresh tube and the RNA was precipitated by adding 0.5 mL isopropanol. The samples were then centrifuged at 12,000 g at 4 °C for ten minutes. The pellet was kept and washed with 1 mL 75% ethanol and the samples were mixed using a vortex, to be thereafter centrifuged at 7,500 g at 4 °C for five minutes. Finally, the RNA pellet was air-dried for ten minutes and solved in RNase-free. Total RNA concentrations were determined spectrophotometrically using the NanoDrop 1000 (Thermo Scientific, Waltham, MA, USA).

mRNA reverse transcription (RT). Complementary DNA (cDNA) was generated from 100 ng mRNA using oligo(dT)12-18 primers, dNTP mix, DTT and the Super-Script III reverse transcriptase as indicated by the manufacturer's instructions (Life Technologies, Carlsbad, CA, USA). RNA was reverse-transcribed using SuperScript III reverse transcriptase and oligo(dT) primers in a 20-µl total reaction volume at 50°C for 60 minutes. The reverse transcription reaction was finished by heating at 70°C for 15 minutes to stop the reaction. Samples were stored at -80°C until further use.

Quantitative real time-PCR amplification (qRT-PCR). Interestingly, qRT-PCR reactions were performed using the QuantStudio 12K Flex Real-Time PCR System (Thermo Fisher Scientific, Waltham, MA, USA) together with the following commercially available gene expression assays: PAX3 (Hs00240950_m1, Life Technologies), PAX7 (Hs00242962_m1, Life Technologies), MYF5 (Hs00929416_g1, Life Technologies), MYOD1 (Hs00159528_m1, Life Technologies), MYOG (Hs01072232_m1, Life Technologies),

MYH7 (Hs00165276_m1, Life Technologies), MYH2 (Hs00430042_m1, Life Technologies) and MYH1 (Hs00428600_m1, Life Technologies). The housekeeping gene glyceraldehyde-3-phosphate dehydrogenase (GAPDH) (Hs99999905_m1, Life Technologies) served as the endogenous control for mRNA gene expression (Table 1) (Esther Barreiro et al., 2019; M. Guitart et al., 2018; Puig-Vilanova, Martínez-Llorens, et al., 2015). Duplicates from all samples were run and the average value was calculated for each study sample. The results obtained from the experiments were collected and analyzed using the ExpressionSuite Software version 1.1 from Applied Biosystems (Thermo Fisher Scientific, Waltham, MA, USA), in which the comparative CT method (2-ΔΔCT) for relative quantification was used as previously reported (Maria Guitart, Lloreta, Mañas-Garcia, & Barreiro, 2018; Livak & Schmittgen, 2001).

Immunoblotting. Protein levels of myostatin were analyzed using immunoblotting procedures as previously described (Esther Barreiro et al., 2019; M. Guitart et al., 2018; Puig-Vilanova, Martínez-Llorens, et al., 2015). Briefly, frozen samples from all experimental groups were homogenized in lysis buffer: 50 mM HEPES, 150 mM NaCl, 100 mM NaF, 10 mM Na pyrophosphate, 5 mM EDTA, 10% glycerol, 0.5% Triton-X, 5 µg/mL aprotinin, 2 µg/mL leupeptin, 100 µg/mL PMSF, and 10 µg/ mL pepstatin A.

Proteins were separated by electrophoresis, transferred to polyvinylidene difluoride (PVDF) membranes, blocked with bovine serum albumin (BSA) and incubated overnight with the corresponding primary antibody: Myostatin (anti-GDG8, Bethyl Laboratories, Montgomery, USA) and the endogenous control glyceraldehyde-3-phosphate dehydrogenase (GAPDH) (anti-GAPDH antibody, Santa Cruz Biotechnology).

Antigens from all samples were detected with horseradish peroxidase (HRP)-conjugated secondary antibodies and a chemiluminescence kit. For each of the antigens, samples from the different groups were always detected in the same picture under identical exposure times.

PVDF membranes were scanned with the Molecular Imager Chemidoc XRS System (Bio–Rad Laboratories, Hercules, CA, USA) using the software Quantity One version 4.6.5 (Bio–Rad Laboratories). Optical densities of specific proteins were quantified using the software Image Lab version 2.0.1 (Bio-Rad Laboratories). Final optical densities obtained in each specific group of subjects and muscle corresponded to the mean values of the different samples (lanes) of each of the antigens studied. In order to validate equal protein loading among various lanes, the glycolytic enzyme GAPDH was used as the protein loading controls in all the immunoblots.

Myostatin identification using immunohistochemical procedures. Myostatin was identified in paraffin sections (three-micrometer thick) from VL muscles corresponding to the three study groups using conventional immunohistochemical procedures as previously described (Puig-Vilanova, Martínez-Llorens, et al., 2015; Puig-Vilanova, Rodriguez, et al., 2015). Following deparaffinization, a pressure cooker containing 10 mM citrate buffer (pH 6.0) was used to boil the sections for 20 minutes. Following a two-hour cooling period, sections were blocked with 6% hydrogen peroxide for 15 min and with a blocking solution (3% BSA, 10% goat serum, and 0.5% triton in PBS) for one hour. The sections were then incubated overnight at 4ºC with the primary antibody: Myostatin (anti-GDG8, Bethyl Laboratories). Slides were then incubated with universal secondary antibody (polystain-1 step kit, HRP for DBA, mouse and rabbit, Neo Biotech, Nanterre, France) for 30 minutes, followed by incubation with the substrate diaminobenzidine (DAB) (DAB kit, Neo Biotech) for five minutes. Hematoxylin counterstaining was performed, and slides were dehydrated and mounted for conventional microscopy. Images of the stained muscle sections were captured with a light microscope (Olympus BX 61, Olympus Corporation) coupled with an image-digitizing camera (Pixera Studio, version 1.0.4, Pixera Corporation).

Statistical Analysis

Normality of the study variables was checked using the Shapiro-Wilk test. All the results are expressed as mean (standard deviation). For the quantitative variables, one-way analysis of variance (ANOVA) with *Tukey's post hoc* analysis was used to adjust for multiple comparisons among the study groups. For the qualitative variables (smoking history), χ^2 test was used to assess differences among the three study groups. A level of significance of $P \leq 0.05$ was established.

RESULTS

Functional and nutritional status of the study subjects

Body composition as measured by BMI and FFMI was significantly reduced in sarcopenic COPD patients compared to non-sarcopenic controls and control subjects (Table 2). Smoking history including the number of packs-year was similar in both groups of COPD patients and significantly differed from that of the controls (never smokers, Table 2). As expected, both groups of COPD patients exhibited severe airflow limitation and a decline in diffusion capacity, especially the sarcopenic patients (Table 2). Moreover, compared to control subjects, exercise tolerance was significantly reduced in both groups of COPD patients, whereas quadriceps muscle strength was significantly lower only in the sarcopenic patients compared to both non-sarcopenic and control subjects (Table 2). Nutritional blood parameters including CRP did not significantly differ among the three study groups of subjects, while fibrinogen levels were significantly greater in both groups of COPD patients than in the controls (Table 2).

Muscle phenotype and damage

The proportions of slow-twitch muscle fibers were significantly lower in the VL of the sarcopenic COPD patients than in the control subjects, while those of the hybrid fibers increased in the limb muscles of both groups of COPD patients (Figure 1A and Table 3).

Furthermore, the proportions of hybrid fibers were significantly greater in the lower limb muscles of the sarcopenic patients than in non-sarcopenic patients (Figure 1A and Table 3). Compared to the controls, the cross-sectional area of slow-twitch fibers was significantly reduced in the VL of both groups of COPD patients. Furthermore, the size of both fast-twitch and hybrid fibers was significantly smaller in muscles of the sarcopenic patients than in both control subjects and non-sarcopenic patients (Figure 1A and Table 3). The proportions of muscle structural abnormalities and internal nuclei counts were significantly greater in the VL of both groups of COPD patients than in control subjects (Figure 1B). Besides, muscle structural abnormalities were also significantly greater in the VL of sarcopenic than in non-sarcopenic COPD patients (Figure 1B). Interestingly, the number of TUNEL-positive nuclei was significantly increased in the VL of both groups of COPD patients compared to those in the control subjects (Figures 2A and 2B). Among all COPD patients, significant correlations were detected between muscle phenotype variables (proportions of slow- and fast-twitch fibers and CSA of type I fibers) and lung function parameters (degree of airway obstruction and diffusion capacity, respectively, Table 4A). Among the COPD patients, significant positive correlations were also detected between CSA of slow and fast-twitch fibers and hybrid fibers and FFMI (Table 4A). Furthermore, among all COPD patients as a whole, quadriceps strength significantly correlated with TUNEL-positive nuclei and muscle abnormalities (Table 4A).

Satellite cells in muscles of COPD patients

The number of quiescent satellite cells as measured by Pax-7+/Myf-5- cells was significantly lower only in VL of the sarcopenic COPD patients than in the control subjects (Figures 3A and 3B). Counts of activated satellite cells (Pax-7+/ Myf-5+) were significantly greater in the VL of both groups of COPD patients than in control subjects (Figures 3A and 3B). Numbers of total satellite cells did not significantly differ among the three study groups (Figures 3A

and 3B). Besides, among all COPD patients as a whole, the number of muscle activated satellite cells inversely correlated with plasma levels of CRP (Table 4A). Specifically, in VL of sarcopenic COPD patients, expression levels of PAX7 and MYOD significantly correlated with the degree of airway obstruction (Table 4B). Moreover, in the same muscles, proportions of slow-twitch fibers significantly correlated with the lung function parameters FEV_1/FVC and DLco (Table 4B).

Expression of muscle regeneration and regulatory markers in COPD patients

Gene expression levels of the regeneration markers Pax-7 and Myf-5 (proliferation phase) and MyoD and MyHCI (differentiation phase) were significantly reduced in the VL of both groups of COPD patients compared to the control subjects (Figure 4A). Protein expression levels of myostatin significantly increased in the VL of the sarcopenic patients compared to both control subjects and non-sarcopenic COPD patients (Figure 4B and 4C). The expression of MyHCIIx was significantly upregulated only in the VL of the sarcopenic COPD patients compared to the control subjects (Figure 4A).

DISCUSSION

In this investigation, the most relevant findings were that in sarcopenic COPD patients with preserved nutritional status and decreased exercise capacity, muscle strength was, indeed, significantly reduced and in the VL of these patients, a significant decline in muscle regeneration potential as measured by the number of Pax-7+/Myf-5- satellite cells, a decrease in slow-twitch fiber type proportions and in the size of both fast-twitch and hybrid fibers, along with a significant rise in both hybrid fibers proportions and muscle structural abnormalities were observed. Importantly, in the limb muscles of both groups of COPD patients, the numbers of internal nuclei, activated satellite cells (Pax-7+/Myf-5+), and TUNEL-positive nuclei were significantly greater than in the controls, while the expression of

markers of early (proliferation phase, Pax-7 and Myf-5) and late (differentiation phase, MyoD and MyHCI) muscle regeneration was downregulated. Levels of the potent negative regulator myostatin increased only in the limb muscles of the sarcopenic COPD patients. Collectively, these findings suggest that markers of regenerative potential in the limb muscles of sarcopenic COPD patients is reduced and myostatin may play a significant role. Moreover, as the rise in muscle damage levels were detected to a greater extent in the VL of the sarcopenic COPD patients (64% greater than in control muscles), such structural alterations are also likely to be involved in the triggering of the muscle regeneration process (Cheung & Rando, 2013; Yin, Price, & Rudnicki, 2013). The most relevant results are discussed below.

Previous investigations have shown that the number of central nuclei, a marker of muscle regeneration, and those of senescent satellite cells were increased in lower limb muscles of COPD patients with different degrees of body composition (M.-E. Thériault et al., 2014; M. E. Thériault et al., 2012).

Among COPD patients, significant correlations were observed between lung function parameters, especially airway obstruction and diffusion capacity and the proportions of slow-twitch fibers, and patients with better lung function parameters were those with a higher proportion of type I fibers. Conversely, proportions and size of type II fibers inversely correlated with the degree of airway obstruction and diffusion capacity. These are relevant findings that suggest that lung function partly contributes to the slow-to-fast fiber type switch in the lower limb muscles of COPD patients as also previously implied (Esther Barreiro et al., 2018; Puig-Vilanova, Martínez-Llorens, et al., 2015; Puig-Vilanova, Rodriguez, et al., 2015). Furthermore, the size of slow- and fast-twitch fibers and that of hybrid fibers also correlated with FFMI, suggesting that lean body mass was associated with a greater CSA of all the muscle fiber types among the COPD patients. In addition, muscle damage and internal nuclei counts were also inversely correlated with isometric strength of the quadriceps muscle of all

the COPD patients. Collectively, these are relevant novel findings that indicate that muscle structure and function are clearly interrelated and should be assessed on routine basis in COPD patient clinics, especially in patients with alterations in their body composition. Another interesting finding in the study was the negative correlation found between CRP plasma levels and the number of activated satellite cells. These results illustrate that systemic inflammation as measured by CRP somehow influenced the process of muscle regeneration as also implied to occur in muscles of COPD patients (Ioannis Vogiatzis et al., 2007).

In the current investigation, a relatively large number of sarcopenic COPD patients of a fairly "young age", with a significant decline in quadriceps muscle function, preserved nutritional status, and altered body composition were carefully recruited. With the aim to elucidate whether muscle regeneration potential may be hampered in the lower limb muscles of sarcopenic COPD patients, two different phenotypes of satellite cells were determined in the present study. As previously characterized (Kuang, Kuroda, Le Grand, & Rudnicki, 2007), sublaminar satellite cells that express Pax-7 but do not express Myf-5 constitute the satellite cell reservoir of a given muscle. In that seminal investigation (Kuang et al., 2007), it was clearly demonstrated that Pax-7+/Myf-5+ satellite cells preferentially differentiate into muscle fibers, whereas Pax-7+/Myf-5- satellite cells contribute to the satellite cell reservoir enlarging this compartment within skeletal muscle. The conclusions from that study (Kuang et al., 2007) were that two different subpopulations of satellite cells were established on the basis of their ability to express Myf-5 (Kuang et al., 2007). As such Pax-7+/Myf-5+ satellite cells were identified as the committed myogenic progenitors, while Pax-7+/Myf-5- satellite cells were defined as the actual stem cells (Kuang et al., 2007).

Importantly, in the present investigation, a significant decline in the number of Pax-7+/Myf-5- satellite cells was detected only in the limb muscles of the sarcopenic COPD patients, but not in those with preserved body composition and normal quadriceps muscle

function. These findings imply that the satellite cell reservoir was hampered in the sarcopenic muscles, which may further jeopardize the process of muscle regeneration. In fact, the proportions of slow-twitch muscle fibers were reduced only in the VL of the sarcopenic COPD patients. Moreover, the size of slow-twitch, fast-twitch, and hybrid myofibers was also significantly smaller in the lower limb muscles of the sarcopenic patients, but not in those with preserved body composition. Additionally, muscle structural abnormalities were even greater in the VL of the sarcopenic COPD patients than in those with no muscle loss. These results, which are very consistent with those obtained in previous investigations (Esther Barreiro et al., 2019; Puig-Vilanova, Martínez-Llorens, et al., 2015; Puig-Vilanova, Rodriguez, et al., 2015), may be partly explained by the poorer regenerative potential detected in the limb muscles of the sarcopenic patients. Proportions of hybrid fibers increased in the limb muscles of both groups of COPD patients and the proportions were even greater in the VL of the sarcopenic patients than in the non-sarcopenic group, while their CSA was smaller in the former patients. These are relevant findings that imply that muscles of COPD patients, especially of the sarcopenic ones, are able to adapt to environmental factors such as inactivity, exercise, or aging (Medler, 2019). Collectively, these events are of paramount importance, since a correct muscle regeneration program is required in order to attain full recovery of muscle mass and function in response to different training modalities. Thus, the current results have potential clinical implications for the design of specific exercise training programs as patients with a defective regenerative potential may be less susceptible to improving their muscle mass and/or function even those with preserved nutritional status.

It is worth noting that the lower limb muscles of both groups of COPD patients experienced the activation of a muscle regeneration program in a similar fashion. In line with this, the number of specific activated satellite cells (Pax-7+/Myf-5+), internal nuclei, and TUNEL-positive nuclei were notably and similarly increased in the VL of both groups of

severe COPD patients compared to those detected in the control muscles. These findings are in line with previous results, in which the process of muscle regeneration was also triggered in the VL of severe COPD patients with a wide range of muscle mass loss (M.-E. Thériault et al., 2014; M. E. Thériault et al., 2012). However, in another study (Menon et al., 2012), the number of satellite cells was similar between COPD patients and healthy controls at baseline. Differences in the level of alterations in body composition compartments and/or muscle function and mass may account for discrepancies encountered among studies (Menon et al., 2012; M.-E. Thériault et al., 2014; M. E. Thériault et al., 2012).

Furthermore, gene expression levels of the early markers of muscle regeneration Pax-7 and Myf-5 were downregulated in the VL of both groups of severe COPD patients compared to the controls. Pax-7 and Myf-5 transcription factors play key roles during the proliferation phase of the muscle regeneration process (M. Guitart et al., 2018; Yin et al., 2013). In keeping with, similar results were also reported in the quadriceps muscle of cachectic COPD patients (Plant et al., 2010; M.-E. Thériault et al., 2014; M. E. Thériault et al., 2012). The downregulation in gene expression of the transcription factors MyoD and Myogenin and of MyHC-I isoform as markers of late muscle differentiation during the regeneration process was another relevant finding in the investigation. These findings are also in line with those previously demonstrated in muscles of patients with advanced COPD (Plant et al., 2010; Puig-Vilanova, Martínez-Llorens, et al., 2015; M.-E. Thériault et al., 2014; M. E. Thériault et al., 2012).

Myostatin, a member of the transforming growth factor beta family, is a negative regulator of muscle growth. Myostatin is also known to inhibit satellite cell and myoblast proliferation through several mechanisms that lead to cell cycle withdrawal (Walsh & Celeste, 2005). Importantly, myostatin levels were significantly greater in the limb muscles of the sarcopenic patients than those detected within the non-sarcopenic patients or the control

subjects. These results are line with previous studies, in which myostatin levels were consistently demonstrated to rise in the lower limb muscles of patients with advanced COPD (Harish et al., 2019; Plant et al., 2010; Puig-Vilanova, Martínez-Llorens, et al., 2015; Walsh & Celeste, 2005). In view of all these findings, it would possible to conclude that myostatin may have interfered with the process of muscle cell proliferation early on during the regeneration process, thus leading to poor muscle growth and development following injury. Hence, this may be another mechanism of muscle mass loss in addition to increased proteolysis and/or apoptosis as also consistently shown in previous investigations (Plant et al., 2010; Puig-Vilanova, Martínez-Llorens, et al., 2015; I Vogiatzis et al., 2010). Nonetheless, elucidation of the precise role and implications of myostatin on muscle regeneration and growth in COPD sarcopenia will have to be definitively confirmed in future investigations.

On the other hand, the reported findings may also have future clinical implications as myostatin blockade using specific antibodies has been shown to partly revert the loss of muscle mass and function in several experimental models (Harish et al., 2019; Iskenderian et al., 2018; St. Andre et al., 2017) and in patients (Burch et al., 2017; Scimeca et al., 2017). Whether anti-myostatin antibodies can also be effectively used in patients with non-muscle diseases such as in sarcopenic COPD will be the matter of research in future investigations. This will shed more light into the implications of myostatin in the muscle regenerative capacity of sarcopenic COPD patients.

Conclusions

In the lower limb muscles of severe COPD patients regardless of the degree of sarcopenia, muscle regeneration process is triggered as identified by satellite cell activation and a rise in internal nuclei counts. Nonetheless, the regenerative potential along with significant alterations in muscle phenotype (slow-to-fast switch phenotype and smaller fast-twitch and hybrid myofibers) and muscle damage were prominently seen in the sarcopenic COPD. A rise

in the muscle growth inhibitor myostatin was also detected only in the VL of the sarcopenic COPD patients, which may further aggravate loss of muscle mass and function in this specific group of patients. These findings have clinical implications as not all COPD patients may equally respond to exercise and/or muscle training modalities and myostatin blockade should be specifically customized to patients with sarcopenia in COPD.

Authors' contributions: Study conception and design: EB, ASM, JMLL; Patient assessment and recruitment and sample collection: ASM, JMLL; Molecular biology analyses: MG; Statistical analyses and data interpretation: MG, ASM, EB; manuscript drafting and intellectual input: EB, ASM, MG, JG, JMLL, DAR; manuscript writing final version: EB.

Ethical publication statement

We confirm that we have read the Journal's position on issues involved in ethical publication and affirm that this report is consistent with those guidelines

Disclosure of conflict of interest

None of the authors has any conflict of interest to disclose

Editorial support

None to declare

REFERENCES

Arentson-Lantz, E. J., English, K. L., Paddon-Jones, D., & Fry, C. S. (2016). Fourteen days of bed rest induces a decline in satellite cell content and robust atrophy of skeletal muscle fibers in middle-aged adults. *Journal of Applied Physiology*, *120*(8), 965–975. https://doi.org/10.1152/japplphysiol.00799.2015

Barreiro, E. (2019). Impact of Physical Activity and Exercise on Chronic Obstructive Pulmonary Disease Phenotypes: The Relevance of Muscle Adaptation. *Archivos de Bronconeumologia*. https://doi.org/10.1016/j.arbres.2019.04.024

Barreiro, E., Ferrer, D., Sanchez, F., Minguella, J., Marin-Corral, J., Martinez-Llorens, J., … Gea, J. (2011). Inflammatory cells and apoptosis in respiratory and limb muscles of patients with COPD. *Journal of Applied Physiology*, *111*(3). https://doi.org/10.1152/japplphysiol.01017.2010

Barreiro, E., Puig-Vilanova, E., Salazar-Degracia, A., Pascual-Guardia, S., Casadevall, C., & Gea, J. (2018). The phosphodiesterase-4 inhibitor roflumilast reverts proteolysis in skeletal muscle cells of patients with COPD cachexia. *Journal of Applied Physiology*, *125*(2), 287–303. https://doi.org/10.1152/japplphysiol.00798.2017

Barreiro, E., Salazar-Degracia, A., Sancho-Muñoz, A., & Gea, J. (2019). Endoplasmic reticulum stress and unfolded protein response profile in quadriceps of sarcopenic patients with respiratory diseases. *Journal of Cellular Physiology*, *234*(7), 11315–11329. https://doi.org/10.1002/jcp.27789

Barreiro, E., Sznajder, J. I., Nader, G. A., & Budinger, G. R. S. (2015). Muscle dysfunction in patients with lung diseases a growing epidemic. *American Journal of Respiratory and Critical Care Medicine*, *191*(6). https://doi.org/10.1164/rccm.201412-2189OE

Burch, P. M., Pogoryelova, O., Palandra, J., Goldstein, R., Bennett, D., Fitz, L., … Morris, C. (2017). Reduced serum myostatin concentrations associated with genetic muscle disease

progression. *Journal of Neurology*, *264*(3), 541–553. https://doi.org/10.1007/s00415-016-8379-6

Cao, L., & Morley, J. E. (2016, August 1). Sarcopenia Is Recognized as an Independent Condition by an International Classification of Disease, Tenth Revision, Clinical Modification (ICD-10-CM) Code. *Journal of the American Medical Directors Association*, Vol. 17, pp. 675–677. https://doi.org/10.1016/j.jamda.2016.06.001

Chacon-Cabrera, A., Fermoselle, C., Urtreger, A. J., Mateu-Jimenez, M., Diament, M. J., de Kier Joffé, E. D. B., … Barreiro, E. (2014). Pharmacological Strategies in Lung Cancer-Induced Cachexia: Effects on Muscle Proteolysis, Autophagy, Structure, and Weakness. *Journal of Cellular Physiology*, *229*(11). https://doi.org/10.1002/jcp.24611

Chacon-Cabrera, A., Lund-Palau, H., Gea, J., & Barreiro, E. (2016). Time-Course of muscle mass loss, damage, and proteolysis in gastrocnemius following unloading and reloading: Implications in chronic diseases. *PLoS ONE*, *11*(10). https://doi.org/10.1371/journal.pone.0164951

Chan, S. M. H., Cerni, C., Passey, S., Seow, H. J., Bernardo, I., van der Poel, C., … Vlahos, R. (2020). Cigarette Smoking Exacerbates Skeletal Muscle Injury without Compromising Its Regenerative Capacity. *American Journal of Respiratory Cell and Molecular Biology*, *62*(2), 217–230. https://doi.org/10.1165/rcmb.2019-0106OC

Cheung, T. H., & Rando, T. A. (2013, June). Molecular regulation of stem cell quiescence. *Nature Reviews Molecular Cell Biology*, Vol. 14, pp. 329–340. https://doi.org/10.1038/nrm3591

Coin, A., Sergi, G., Minicuci, N., Giannini, S., Barbiero, E., Manzato, E., … Enzi, G. (2008). Fat-free mass and fat mass reference values by dual-energy X-ray absorptiometry (DEXA) in a 20-80 year-old Italian population. *Clinical Nutrition*, *27*(1), 87–94. https://doi.org/10.1016/j.clnu.2007.10.008

Gea, J., & Martínez-Llorens, J. (2019). Muscle Dysfunction in Chronic Obstructive Pulmonary Disease: Latest Developments. *Archivos de Bronconeumologia*, *55*(5), 237–238. https://doi.org/10.1016/j.arbres.2018.07.016

Gea, J., Pascual, S., Castro-Acosta, A., Hernández-Carcereny, C., Castelo, R., Márquez-Martín, E., … Anexo. Miembros del grupo BIOMEPOC. (2019). The BIOMEPOC Project: Personalized Biomarkers and Clinical Profiles in Chronic Obstructive Pulmonary Disease. *Archivos de Bronconeumologia*, *55*(2), 93–99. https://doi.org/10.1016/j.arbres.2018.07.026

Guitart, M., Lloreta, J., Mañas-Garcia, L., & Barreiro, E. (2018). Muscle regeneration potential and satellite cell activation profile during recovery following hindlimb immobilization in mice. *Journal of Cellular Physiology*, *233*(5). https://doi.org/10.1002/jcp.26282

Guitart, M., Lloreta, J., Mañas-Garcia, L., & Barreiro, E. (2018). Muscle regeneration potential and satellite cell activation profile during recovery following hindlimb immobilization in mice. *Journal of Cellular Physiology*, *233*(5), 4360–4372. https://doi.org/10.1002/jcp.26282

Harish, P., Malerba, A., Lu-Nguyen, N., Forrest, L., Cappellari, O., Roth, F., … Dickson, G. (2019). Inhibition of myostatin improves muscle atrophy in oculopharyngeal muscular dystrophy (OPMD). *Journal of Cachexia, Sarcopenia and Muscle*, *10*(5), 1016–1026. https://doi.org/10.1002/jcsm.12438

Iskenderian, A., Liu, N., Deng, Q., Huang, Y., Shen, C., Palmieri, K., … Ehmann, D. E. (2018). Myostatin and activin blockade by engineered follistatin results in hypertrophy and improves dystrophic pathology in mdx mouse more than myostatin blockade alone. *Skeletal Muscle*, *8*(1). https://doi.org/10.1186/s13395-018-0180-z

Jaitovich, A., & Barreiro, E. (2018). Skeletal muscle dysfunction in chronic obstructive

pulmonary disease what we know and can do for our patients. *American Journal of Respiratory and Critical Care Medicine*, *198*(2). https://doi.org/10.1164/rccm.201710-2140CI

Jones, N. L., Makrides, L., Hitchcock, C., Chypchar, T., & McCartney, N. (1985). Normal standards for an incremental progressive cycle ergometer test. *American Review of Respiratory Disease*, *131*(5), 700–708. https://doi.org/10.1164/arrd.1985.131.5.700

Kuang, S., Kuroda, K., Le Grand, F., & Rudnicki, M. A. (2007). Asymmetric self-renewal and commitment of satellite stem cells in muscle. *Cell*, *129*(5), 999–1010. https://doi.org/10.1016/j.cell.2007.03.044

Kwan, H. Y., Maddocks, M., Nolan, C. M., Jones, S. E., Patel, S., Barker, R. E., … Man, W. D. C. (2019). The prognostic significance of weight loss in chronic obstructive pulmonary disease-related cachexia: a prospective cohort study. *Journal of Cachexia, Sarcopenia and Muscle*, *10*(6), 1330–1338. https://doi.org/10.1002/jcsm.12463

Livak, K. J., & Schmittgen, T. D. (2001). Analysis of relative gene expression data using real-time quantitative PCR and the 2-ΔΔCT method. *Methods*, *25*(4), 402–408. https://doi.org/10.1006/meth.2001.1262

Marquis, K., Debigaré, R., Lacasse, Y., LeBlanc, P., Jobin, J., Carrier, G., & Maltais, F. (2002). Midthigh muscle cross-sectional area is a better predictor of mortality than body mass index in patients with chronic obstructive pulmonary disease. *American Journal of Respiratory and Critical Care Medicine*, *166*(6), 809–813. https://doi.org/10.1164/rccm.2107031

Martínez-Llorens, J., Casadevall, C., Lloreta, J., Orozco-Levi, M., Barreiro, E., Broquetas, J., & Gea, J. (2008). [Activation of satellite cells in the intercostal muscles of patients with chronic obstructive pulmonary disease]. *Archivos de Bronconeumologia*, *44*(5), 239–244. Retrieved from http://www.ncbi.nlm.nih.gov/pubmed/18448014

Medler, S. (2019, November 29). Mixing it up: The biological significance of hybrid skeletal muscle fibers. *Journal of Experimental Biology*, Vol. 22, p. 1OBITUARY. https://doi.org/10.1242/jeb.200832

Menon, M. K., Houchen, L., Singh, S. J., Morgan, M. D., Bradding, P., & Steiner, M. C. (2012). Inflammatory and satellite cells in the quadriceps of patients with COPD and response to resistance training. *Chest*, *142*(5), 1134–1142. https://doi.org/10.1378/chest.11-2144

Miravitlles, M., Soler-Cataluña, J. J., Calle, M., Molina, J., Almagro, P., Quintano, J. A., … Ancochea, J. (2017). Spanish Guidelines for Management of Chronic Obstructive Pulmonary Disease (GesEPOC) 2017. Pharmacological Treatment of Stable Phase. *Archivos de Bronconeumologia*, *53*(6), 324–335. https://doi.org/10.1016/j.arbres.2017.03.018

Muscaritoli, M., Anker, S. D., Argilés, J., Aversa, Z., Bauer, J. M., Biolo, G., … Sieber, C. C. (2010). Consensus definition of sarcopenia, cachexia and pre-cachexia: Joint document elaborated by Special Interest Groups (SIG) " cachexia-anorexia in chronic wasting diseases" and " nutrition in geriatrics." *Clinical Nutrition*, *29*(2), 154–159. https://doi.org/10.1016/j.clnu.2009.12.004

Ohno, Y., Matsuba, Y., Hashimoto, N., Sugiura, T., Ohira, Y., Yoshioka, T., & Goto, K. (2016). Suppression of myostatin stimulates regenerative potential of injured antigravitational soleus muscle in mice under unloading condition. *International Journal of Medical Sciences*, *13*(9), 680–685. https://doi.org/10.7150/ijms.16267

Plant, P. J., Brooks, D., Faughnan, M., Bayley, T., Bain, J., Singer, L., … Batt, J. (2010). Cellular markers of muscle atrophy in chronic obstructive pulmonary disease. *American Journal of Respiratory Cell and Molecular Biology*, *42*(4), 461–471. https://doi.org/10.1165/rcmb.2008-0382OC

Puig-Vilanova, E., Martínez-Llorens, J., Ausin, P., Roca, J., Gea, J., & Barreiro, E. (2015). Quadriceps muscle weakness and atrophy are associated with a differential epigenetic profile in advanced COPD. *Clinical Science*, *128*(12). https://doi.org/10.1042/CS20140428

Puig-Vilanova, E., Rodriguez, D. A., Lloreta, J., Ausin, P., Pascual-Guardia, S., Broquetas, J., … Barreiro, E. (2015). Oxidative stress, redox signaling pathways, and autophagy in cachectic muscles of male patients with advanced COPD and lung cancer. *Free Radical Biology and Medicine*, *79*. https://doi.org/10.1016/j.freeradbiomed.2014.11.006

Ricciardi, R. (2006). Sedentarism: a concept analysis. *Nursing Forum*, *40*(3), 79–87. https://doi.org/10.1111/j.1744-6198.2005.00021.x

Roca, J., Burgos, F., Barberà, J. A., Sunyer, J., Rodriguez-Roisin, R., Castellsagué, J., … Clausen, J. L. (1998). Prediction equations for plethysmographic lung volumes. *Respiratory Medicine*, *92*(3), 454–460. https://doi.org/10.1016/s0954-6111(98)90291-8

Roca, J., Burgos, F., Sunyer, J., Saez, M., Chinn, S., Antó, J. M., … Burney, P. (1998). References values for forced spirometry. Group of the European Community Respiratory Health Survey. *The European Respiratory Journal*, *11*(6), 1354–1362. Retrieved from http://www.ncbi.nlm.nih.gov/pubmed/9657579

Roca, J., Vargas, C., Cano, I., Selivanov, V., Barreiro, E., Maier, D., … Gomez-Cabrero, D. (2014). Chronic Obstructive Pulmonary Disease heterogeneity: Challenges for health risk assessment, stratification and management. *Journal of Translational Medicine*, *12*. https://doi.org/10.1186/1479-5876-12-S2-S3

Rodriguez, D. A., Kalko, S., Puig-Vilanova, Ø., Perez-Olabarría, M., Falciani, F., Gea, J., … Roca, J. (2012). Muscle and blood redox status after exercise training in severe COPD patients. *Free Radical Biology and Medicine*, *52*(1), 88–94. https://doi.org/10.1016/j.freeradbiomed.2011.09.022

Salazar-Degracia, A., Blanco, D., Vilà-Ubach, M., Biurrun, G., Solórzano, C. O., Montuenga, L. M., & Barreiro, E. (2016). Phenotypic and metabolic features of mouse diaphragm and gastrocnemius muscles in chronic lung carcinogenesis: Influence of underlying emphysema. *Journal of Translational Medicine*, *14*(1). https://doi.org/10.1186/s12967-016-1003-9

Scimeca, M., Piccirilli, E., Mastrangeli, F., Rao, C., Feola, M., Orlandi, A., … Tarantino, U. (2017). Bone Morphogenetic Proteins and myostatin pathways: Key mediator of human sarcopenia. *Journal of Translational Medicine*, *15*(1). https://doi.org/10.1186/s12967-017-1143-6

Seymour, J. M., Spruit, M. A., Hopkinson, N. S., Natanek, S. A., Man, W. D.-C., Jackson, A., … Wouters, E. F. M. (2010). The prevalence of quadriceps weakness in COPD and the relationship with disease severity. *The European Respiratory Journal*, *36*(1), 81–88. https://doi.org/10.1183/09031936.00104909

Shrestha, B., & Dunn, L. (2020). The Declaration of Helsinki on Medical Research involving Human Subjects: A Review of Seventh Revision. *Journal of Nepal Health Research Council*, *17*(4), 548–552. https://doi.org/10.33314/jnhrc.v17i4.1042

Shrikrishna, D., Patel, M., Tanner, R. J., Seymour, J. M., Connolly, B. A., Puthucheary, Z. A., … Hopkinson, N. S. (2012). Quadriceps wasting and physical inactivity in patients with COPD. *European Respiratory Journal*, *40*(5), 1115–1122. https://doi.org/10.1183/09031936.00170111

Snijders, T., Wall, B. T., Dirks, M. L., Senden, J. M. G., Hartgens, F., Dolmans, J., … Van Loon, L. J. C. (2014). Muscle disuse atrophy is not accompanied by changes in skeletal muscle satellite cell content. *Clinical Science*, *126*(8), 557–566. https://doi.org/10.1042/CS20130295

St. Andre, M., Johnson, M., Bansal, P. N., Wellen, J., Robertson, A., Opsahl, A., … Owens, J.

(2017). A mouse anti-myostatin antibody increases muscle mass and improves muscle strength and contractility in the mdx mouse model of Duchenne muscular dystrophy and its humanized equivalent, domagrozumab (PF-06252616), increases muscle volume in cynomolgus monkeys. *Skeletal Muscle*, *7*(1). https://doi.org/10.1186/s13395-017-0141-y

Suetta, C., Frandsen, U., Mackey, A. L., Jensen, L., Hvid, L. G., Bayer, M. L., … Kjaer, M. (2013). Ageing is associated with diminished muscle re-growth and myogenic precursor cell expansion early after immobility-induced atrophy in human skeletal muscle. *Journal of Physiology*, *591*(15), 3789–3804. https://doi.org/10.1113/jphysiol.2013.257121

Swallow, E. B., Reyes, D., Hopkinson, N. S., Man, W. D. C., Porcher, R., Cetti, E. J., … Polkey, M. I. (2007). Quadriceps strength predicts mortality in patients with moderate to severe chronic obstructive pulmonary disease. *Thorax*, *62*(2), 115–120. https://doi.org/10.1136/thx.2006.062026

Thériault, M.-E., Paré, M.-È., Lemire, B. B., Maltais, F., & Debigaré, R. (2014). Regenerative defect in vastus lateralis muscle of patients with chronic obstructive pulmonary disease. *Respiratory Research*, *15*(1), 35. https://doi.org/10.1186/1465-9921-15-35

Thériault, M. E., Paré, M. È., Maltais, F., & Debigaré, R. (2012). Satellite cells senescence in limb muscle of severe patients with COPD. *PLoS ONE*, *7*(6), e39124. https://doi.org/10.1371/journal.pone.0039124

Vogelmeier, C. F., Criner, G. J., Martínez, F. J., Anzueto, A., Barnes, P. J., Bourbeau, J., … Agustí, A. (2017). Global Strategy for the Diagnosis, Management, and Prevention of Chronic Obstructive Lung Disease 2017 Report: GOLD Executive Summary. *Archivos de Bronconeumologia*, *53*(3), 128–149. https://doi.org/10.1016/j.arbres.2017.02.001

Vogiatzis, I., Simoes, D. C. M., Stratakos, G., Kourepini, E., Terzis, G., Manta, P., … Zakynthinos, S. (2010). Effect of pulmonary rehabilitation on muscle remodelling in cachectic patients with COPD. *The European Respiratory Journal*, *36*(2), 301–310.

https://doi.org/10.1183/09031936.00112909

Vogiatzis, I., Stratakos, G., Simoes, D. C. M., Terzis, G., Georgiadou, O., Roussos, C., & Zakynthinos, S. (2007). Effects of rehabilitative exercise on peripheral muscle TNFα, IL-6, IGF-I and MyoD expression in patients with COPD. *Thorax*, *62*(11), 950–956. https://doi.org/10.1136/thx.2006.069310

Walsh, F. S., & Celeste, A. J. (2005). Myostatin: A modulator of skeletal-muscle stem cells. *Biochemical Society Transactions*, *33*(6), 1513–1517. https://doi.org/10.1042/BST20051513

Wurtzel, C. N. W., Gumucio, J. P., Grekin, J. A., Khouri, R. K., Russell, A. J., Bedi, A., & Mendias, C. L. (2017). Pharmacological inhibition of myostatin protects against skeletal muscle atrophy and weakness after anterior cruciate ligament tear. *Journal of Orthopaedic Research*, *35*(11), 2499–2505. https://doi.org/10.1002/jor.23537

Yin, H., Price, F., & Rudnicki, M. A. (2013). Satellite cells and the muscle stem cell niche. *Physiological Reviews*, *93*(1), 23–67. https://doi.org/10.1152/physrev.00043.2011

Table 1. Gene expression assays used to assess muscle regeneration marker levels

Gene symbol	Assay ID	Genbank accession number
Muscle regeneration markers		
PAX3	Hs00240950_m1	NM_000438.5
		NM_013942.4
		NM_181457.3
		NM_181458.3
		NM_181459.3
		NM_181460.3
		NM_181461.3

PAX7	Hs00242962_m1	NM_001135254.1 NM_002584.2 NM_013945.2
MYF5	Hs00929416_g1	NM_005593.2
MYOD1	Hs00159528_m1	NM_002478.4
MYOG	Hs01072232_m1	NM_002479.5
MYH7	Hs00165276_m1	NM_000257.3
MYH2	Hs00430042_m1	NM_001100112.1 NM_017534.5
MYH1	Hs00428600_m1	NM_005963.3
GAPDH	Hs99999905_m1	NM_001289746.1 NM_002046. 5

Abbreviations: ID, identification; Hs, homo sapiens; m1, multi-exonic gene assay does not detect genomic DNA; g1, multi-exonic gene assay may detect genomic DNA if present in the sample; NM, mRNA RefSeq database category; PAX3, paired box gene 3; PAX7, paired box gene 7; MYF5, Myogenic factor 5; MYOD1, myogenic differentiation 1; MYOG, myogenin; MYH7, myosin heavy chain 7; MYH2, myosin heavy chain 2; MYH1, myosin heavy chain 1; and GAPDH, glyceraldehyde-3-phosphate dehydrogenase.

Table 2. Clinical characteristics of the COPD patients and control subjects

		COPD patients	
	Control subjects	**Non-sarcopenic**	**Sarcopenic**
	N=13	**N=19**	**N=26**
Anthropometry			
Age (years)	66 (5)	65 (7)	62 (8)
Body weight (kg)	72 (15)	75 (11)	52 (9) **,###
Males/females	6/7	14/5	11/15
BMI (kg/m^2)	27 (4)	28 (2)	19 (3) #
FFMI (kg/m^2)	17 (2)	18 (1)	14 (1) ***,###
Smoking history			
Active, N (%)	0 (0)	15 (79) ***	16 (62) ***
Ex-smoker, N (%)	0 (0)	4 (21) ***	10 (38) ***

Never smoker, N (%)	13 (100)	0 (0) ***	0 (0) ***
Packs-year	0 (0)	61 ***	55 ***
Lung function testing			
FEV1, % predicted	97 (14)	36 (11) ***	34 (11) ***
FVC, % predicted	98 (12)	67 (15) ***	70 (16) ***
FEV_1/FVC	76 (6)	42 (10) ***	38 (12) ***
RV, % predicted	112 (14)	185 (43) ***	224 (52) ***,#
TLC, % predicted	97 (7)	108 (14)	122 (18) ***,#
RV/TLC	43 (9)	61 (9) ***	65 (8) ***
DLco, % predicted	91 (6)	46 (16) ***	35 (13) ***
KCO, % predicted	93 (19)	49 (16) ***	40 (14) ***
PaO_2 (KPa)	NA	9.4 (2.0)	8.6 (4.0)
$PaCO_2$ (KPa)	NA	5.5 (0.5)	5.8 (1.0)
Exercise capacity and muscle function			
VO_2 max (% pred)	120 (32)	59 (18) ***	54 (24) ***
6-min walking distance (m)	523 (55)	421 (79) **	443 (64) **
QMVC (Kg)	42 (13)	40 (12)	31 (7) **,##
QMVC (Kg)/FFM (Kg)	0.9 (0.1)	0.8 (0.2)	0.8 (0.2)
Blood parameters			
Albumin (g/dL)	4.6 (0.2)	4.5 (0.3)	4.6 (0.2)
Total proteins (g/dL)	7.1 (0.3)	7.0 (0.4)	7.1 (0.6)
CRP (mg/dL)	0.3 (0.3)	0.5 (0.3)	0.3 (0.3)
Fibrinogen (mg/dL)	355 (69)	469 (87) **	418 (76) *
GSV (mm/h)	10 (7)	17 (13)	10 (11)

Values are expressed as mean (standard deviation).

Abbreviations: COPD, chronic obstructive pulmonary disease; N, number of patients; m, meters; BMI, body mass index; FFMI, fat-free mass index; FFM, fat-free mass, kg, kilograms; FEV_1, forced expiratory volume in one second; pred, predicted; FVC, forced vital capacity; RV, residual volume; TLC, total lung capacity; DLco, carbon monoxide transfer; KCO, Krough transfer factor; PaO_2, arterial oxygen partial pressure; $PaCO_2$, arterial carbon dioxide partial pressure; VO_2 peak, peak exercise oxygen uptake; QMVC, quadriceps maximum voluntary contraction; QMVC/FFM, quadriceps maximum voluntary contraction/fat-free mass; g, grams; dL, deciliter; mg, miligrams.; CRP, C-reactive protein; GSV, globular sedimentation velocity; mm, millimeters; h, hour. Statistical significance: *, $p<0.05$, **, $p<0.01$, ***, $p<0.001$ between any of the groups of COPD patients and the control subjects; #, $p<0.05$, ##, $p<0.01$, ###, $p<0.001$ between sarcopenic and non-sarcopenic COPD patients.

Table 3. Fiber type characteristics of the vastus lateralis in the study subjects

		COPD patients	
	Control subjects	**Non-sarcopenic**	**Sarcopenic**
Fiber Type I proportion (%)	33.0 (5.9)	28.7 (13.2)	26.6 (9.4)*
Fiber type II proportion (%)	65.2 (5.6)	64.3 (13.7)	63.0 (10.5)
Hybrid fiber proportion (%)	1.8 (1.7)	6.9 (4.1)**	10.3 (6.7)**,#
Type I Fibers CSA, μm^2	3589 (1260)	2678 (540)*	2085 (475)***
Type II Fibers CSA, μm^2	2800 (1322)	2819 (851)	1503 (395)**, ##
Hybrid fibers CSA, μm^2	2777 (1534)	2608 (910)	2042 (827)***, #

Mean values and standard deviation of the proportions and sizes (cross-sectional areas) in the VL of both groups of COPD patients and the control subjects. Definition of abbreviations: N, sample size; CSA, cross sectional area.

Statistical significance: *, p<0.05, **, p<0.01 and ***, p<0.001 between any of the groups of COPD patients and the control subjects; #, p<0.05, ## p<0.01 between sarcopenic and non-sarcopenic COPD patients.

Table 4A. Significant correlations of the study variables among all the study COPD patients

	FEV_1/FVC	FEV_1	DL_{CO}	KCO	FFMI	QMVC	CRP
TUNEL						r = 0.432 P = 0.019	
Abnormal fraction						r = -0.470 P = 0.010	
Internal nuclei						r = -0.367 P = 0.036	
Fiber Type I %	r = 0.523	r = 0.418	r = 0.543				

	P = 0.003	P = 0.021	P = 0.003			
Fiber Type II %	r = -0.428	r = -0.444	r = -0.467			
	P = 0.003	P = 0.007	P = 0.006			
Type I Fibers CSA			r = 0.460	r = 0.444	r = 0.493	
			P = 0.018	P = 0.020	P = 0.007	
Type II Fibers CSA					r = 0.673	
					P = 0.000	
Hybrid fibers CSA					r = 0.415	
					P = 0.018	
Pax-7+/Myf-5+						r = -0.426
						P = 0.015

In the table, units have been omitted for the sake of clarity, as they are already described in the corresponding figures and tables. COPD, chronic obstructive pulmonary disease; FEV1, forced expiratory volume in 1 s; FVC, forced vital capacity; DLco, carbon monoxide transfer; KCO, Krough transfer factor; FFMI, fat-free mass index; QMVC, quadriceps maximum voluntary contraction; CRP, C-reactive protein; CSA, cross sectional area.

Table 4B. Significant correlations of the study variables among sarcopenic COPD patients

	FEV_1/FVC	DL_{CO}
Fiber Type I %	r = 0.504	r = 0.474
	P = 0.047	P = 0.087
PAX7	r = 0.537	
	P = 0.015	
MYOD	r = 0.703	
	P = 0.000	

For the sake of clarity in the table, units have been omitted, as they are already being shown in the corresponding figures and tables. COPD, chronic obstructive pulmonary disease; FEV1, forced expiratory volume in 1 s; FVC, forced vital capacity; DLco, carbon monoxide transfer; CSA, cross sectional area.

FIGURE LEGENDS

Figure 1: (a) Representative images of VL cross-sectional histological preparations. Myofibers positively stained for slow-twitch antibody appear in brown color in the left panels. Myofibers positively stained for fast-twitch antibody appear in brown color in the right panels. Hybrid myofibers are positively stained for slow-twitch and fast-twitch antibodies (black arrows). (b) Mean values and standard deviation of muscle abnormalities: as measured by total abnormal fraction and proportions of internal nuclei and inflammatory cells identified in the VL of control subjects (white bars) and in both non-sarcopenic (grey bars) and sarcopenic COPD patients (black bars). Statistical significance: *$p \leq 0.05$, **$p \leq 0.01$, ***$p \leq 0.001$ between any of the COPD patient groups and the control subjects; $^{\#}p \leq 0.05$ between sarcopenic and non-sarcopenic COPD patients.

Figure 2: (a) Representative images of TUNEL-positively stained nuclei (brown, black arrows) and TUNEL-negative nuclei (green, dotted arrows) in the VL. (b) Mean values and standard deviation of the percentage of positively stained nuclei for the TUNEL assay in the VL of the control subjects (white bars), non-sarcopenic COPD patients (grey bars) and sarcopenic COPD patients (black bars). Statistical significance: ***$p \leq 0.001$ between any of the groups of COPD patients and the control subjects.

Figure 3: (a) Mean values and standard deviation of Pax-7+/Myf-5- (quiescent), Pax-7+/Myf-5+ (activated) and total satellite cell counts per myofiber in the VL of control subjects (white bars) and in both non-sarcopenic COPD patients (grey bars) and sarcopenic COPD patients (black bars). Statistical significance: *$p \leq 0.05$, **$p \leq 0.01$ between any of the groups of COPD patients and the control subjects. (b) Representative images of immunofluorescence staining of DAPI (left panels), Pax-7 (middle-left panels), Myf-5 (middle-right panels) and

cells positively stained for both Pax-7 and Myf-5 markers (right panels) in muscles of control subjects and in both non-sarcopenic and sarcopenic COPD patients. Triangle arrows indicate Pax-7 positive cells (quiescent satellite cells) and thin arrows indicate double-stained nuclei for both Pax-7 and Myf-5 positive cells (activated satellite cells).

Figure 4: (a) Mean values and standard deviation (relative expression) of genes of muscle structure and regeneration in the VL of the control subjects (white bars), non-sarcopenic COPD (grey bars) and sarcopenic COPD patients (black bars). Statistical significance: *$p \leq 0.05$, **$p \leq 0.01$, ***$p \leq 0.001$ between any of the groups of COPD patients and the control subjects. (b) Mean values and standard deviation of myostatin protein, measured in optical densities (OD) using arbitrary units (a.u.) in the VL of the control subjects (white bars) and in both non-sarcopenic (grey bars) and sarcopenic COPD patients (black bars). Statistical significance: **$p \leq 0.01$ between sarcopenic COPD patients and the control subjects; $^{\#}p \leq 0.05$ between sarcopenic and non-sarcopenic COPD patients. (c) Representative images of VL cross-sectional histological preparations. Myostatin protein appears in brown color.

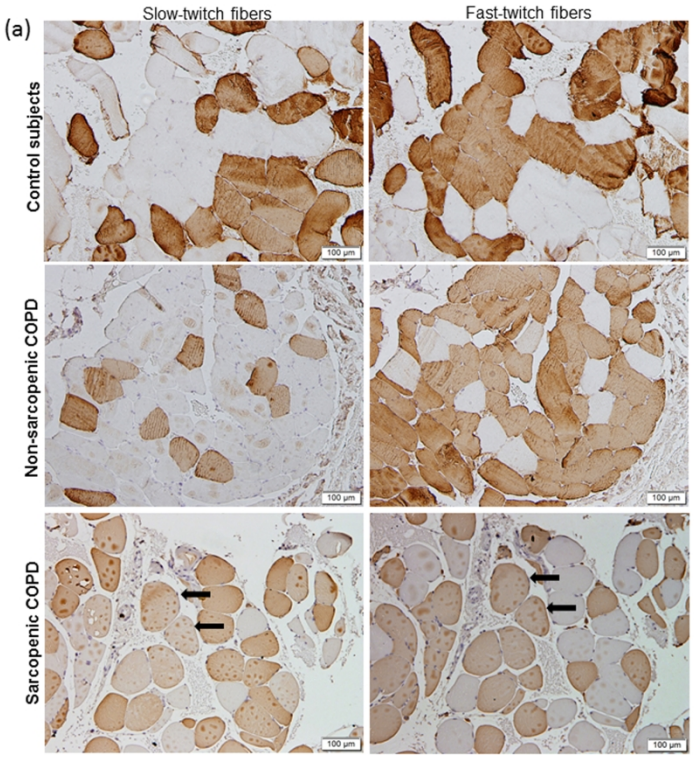

FIGURE 1A

254x190mm (300 x 300 DPI)

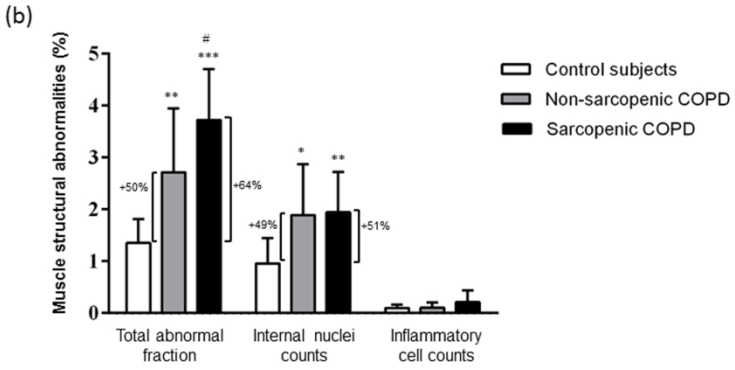

FIGURE 1B

254x190mm (300 x 300 DPI)

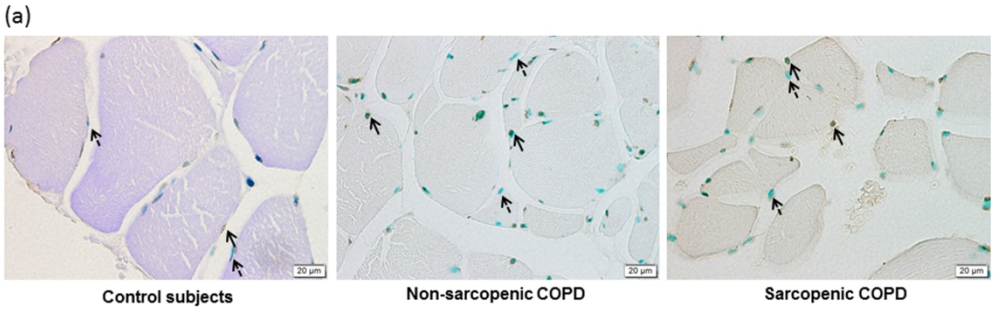

FIGURE 2A

254x190mm (300 x 300 DPI)

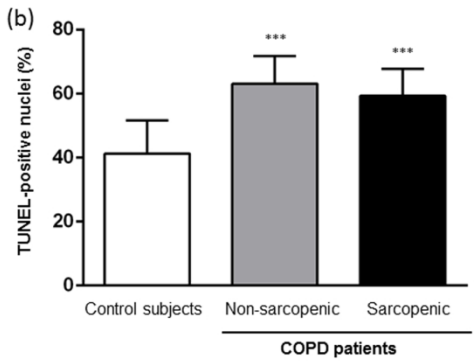

FIGURE 2B

254x190mm (300 x 300 DPI)

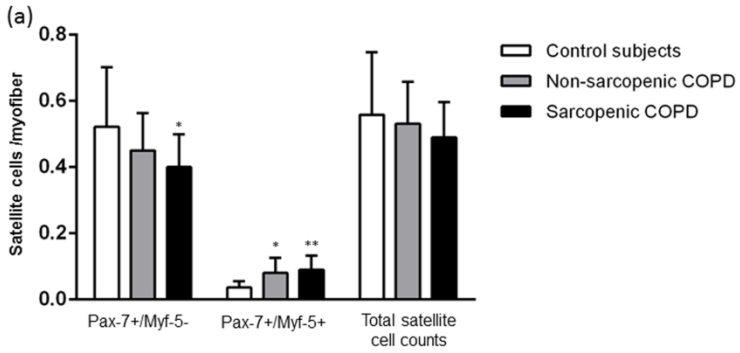

FIGURE 3A

254x190mm (300 x 300 DPI)

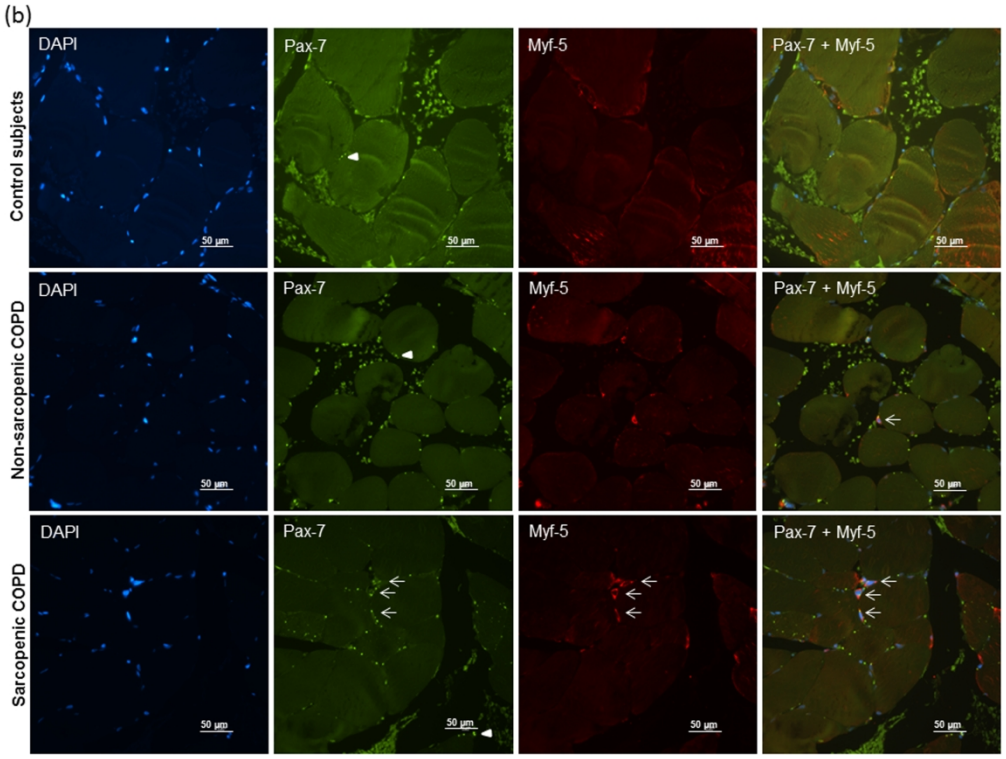

FIGURE 3B

254x190mm (300 x 300 DPI)

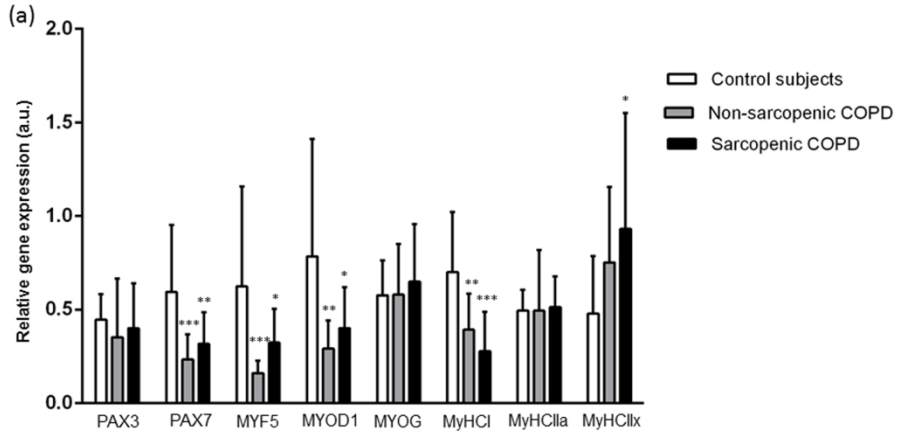

FIGURE 4A

254x190mm (300 x 300 DPI)

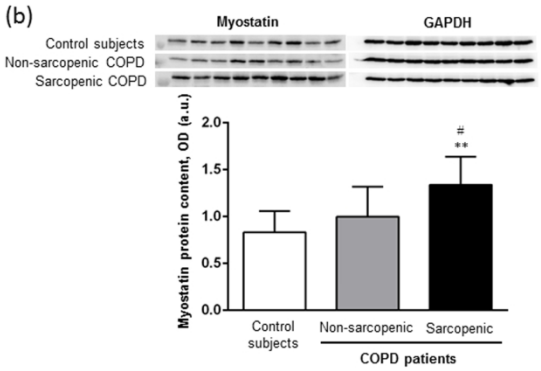

FIGURE 4B

254x190mm (300 x 300 DPI)

(c)

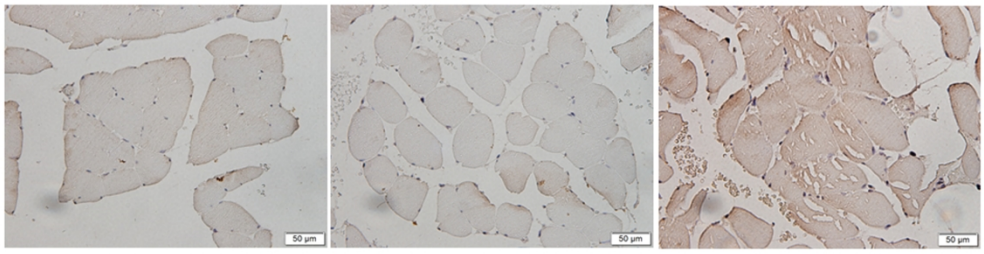

FIGURE 4C

254x190mm (300 x 300 DPI)